AN IMAGE PROCESSING APPROACH FOR UNDERDETERMINED BLIND SEPARATION OF NONSTATIONARY SOURCES

K. Abed–Meraim†, *N. Linh–Trung*†, *V. Sucic*††, *F. Tupin*† *and B. Boashash*††

† Signal & Image Processing Department, Telecom Paris (ENST), Paris, France

†† Signal Processing Research Centre, Queensland University of Technology, Australia

ABSTRACT

This paper presents a new approach for blind separation of nonstationary frequency–modulated (FM) sources in the underdetermined case (i.e., more sources than sensors) using their time–frequency distributions (TFDs). The underlying idea of the proposed blind source separation (BSS) method is based on the observation that a monocomponent FM signal is represented by a linear feature corresponding to the 'energy concentration points' in the time–frequency (TF) image. Therefore, we propose to adapt an existing 'road network extraction' method [Tupin *et al.* (1998)] for the detection and separation of the source signal components from the spatially averaged TF image of their mixtures. The sources spatial signatures are then used to group together (classify) the components of the same source (or equivalently, the same spatial direction). Simulation examples are provided to assess the performance of proposed algorithm in various scenarios.

1. INTRODUCTION

Blind source separation (BSS) is a fundamental technique in array signal processing aiming at recovering unobserved signals or sources from observed mixtures (typically, the outputs of a multisensor array), exploiting usually the assumption of mutual independence between the signals [1]. The term 'blind' indicates that neither the structure of the mixtures nor the source signals are known to the receivers.

BSS has attracted a wide attention over the past decade and been signified by an ongoing series of conferences [2]. Useful reviews of BSS theories and algorithms can be found in [1, 3–6]. BSS has many applications in areas involving processing of multi-sensor array signals where spatial diversity is exploited.

In the case of *nonstationary* signals, a time–frequency (TF) based approach was introduced in [7, 8] by defining the spatial time–frequency distribution (STFD), which combines both TF diversity and spatial diversity. The benefits of STFD in an environment of nonstationary signals is the direct exploitation of the information brought by the nonstationarity of the signals. A challenging problem in this field is the source separation in situations where there are more sources than sensors [10]. This difficult problem, known as the *underdetermined BSS* (UBSS), has recently been studied in [10–13] where discrete sources were treated; and in [14] where disjoint orthogonality of the short–time Fourier transform was exploited.

Recently, a new UBSS method based on the TF domain orthogonality concept has been proposed [15]. This method exploits the fact that all the TF auto–term points of the same source have the same principal eigenvector representing the source direction. Thus, by clustering all the TF auto–term points into different groups, i.e. source TF signatures, one is able to recover the original source using a TF synthesis algorithm.

A major problem of the algorithm proposed in [15] is that the TF auto–term selection process does not, in practice, cleanly remove all the undesired cross–term points. As a consequence, the original sources, though successfully recovered, contain some undesired artifacts. This algorithm was improved by using other reduced–interference TFD distributions for suppressing the cross–terms [15]. In this paper, we want to further improve the above algorithm from an image processing point of view by adding a component–extraction procedure.

The component–extraction procedure can be seen as the detection of the linear features in the TF image of the signal. This problem has been widely addressed in image processing field, specially for road detection applications with aerial or satellite images. Therefore, classical image processing tools can be easily adapted to our component–extraction objective.

2. BACKGROUND

2.1. Signal model and assumptions

Assume that an n–dimensional vector $\mathbf{s}(t) = [s_1(t), \ldots, s_n(t)]^T \in \mathbb{C}^{(n\times 1)}$ corresponds to n nonstationary complex source signals $s_i(t)$, $i = 1, \ldots, n$. The source signals are transmitted through a medium so that an array of m sensors picks up a set of mixed signals represented by an m–dimensional vector $\mathbf{x}(t) = [x_1(t), \ldots, x_m(t)]^T \in \mathbb{C}^{(m\times 1)}$. Consider an instantaneous linear mixture medium, the ob-

served signals can, then, be modeled as:

$$\mathbf{x}(t) = \mathbf{A}\mathbf{s}(t) + \boldsymbol{\eta}(t), \tag{1}$$

where $\mathbf{A} \in \mathbb{C}^{(m\times n)}$ is called the mixing matrix and $\boldsymbol{\eta}(t) = [\eta_1(t), \eta_2(t), \ldots, \eta_m(t)]^T \in \mathbb{C}^{(m\times 1)}$ is the observation noise vector. For the UBSS problem, i.e. $n > m$, the mixing matrix $\mathbf{A}$ is not (left) invertible.

Here, the sources are assumed to be multicomponent FM signals. By a multicomponent signal, we mean a signal whose TF representation presents multiple ridges in the time-frequency plane. Analytically, the k-th source may be defined as,

$$s_k(t) = \sum_{l=1}^{M_k} s_{k,l}(t) \tag{2}$$

where each component $s_{k,l}(t)$, of the form

$$s_{k,l}(t) = a_{k,l}(t)\, e^{j\phi_{k,l}(t)}, \tag{3}$$

is assumed to have only one ridge in the TF plane. An example of a multicomponent signal, consisting of three components, is displayed in Figure 1.

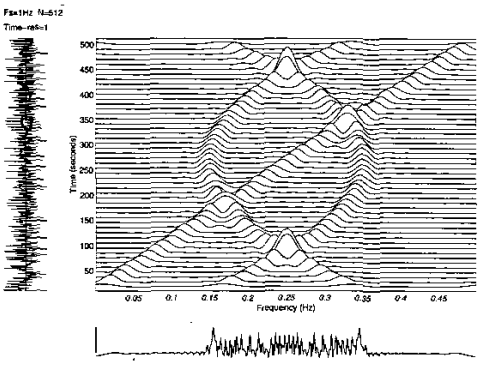

Figure 1: A time–frequency distribution of a multicomponent signal.

2.2. TFD–based Algorithm for UBSS

In [15], a TFD–based algorithm was proposed to solve the UBSS problem. This algorithm achieves the separation based mainly on the assumption of source TF orthogonality that allows an explicit use of the nonstationarity property. The algorithm is composed of four main steps (see [15] for more details):

- Computation of the spatial time–frequency distribution (STFD) matrices of the observations, and noise thresholding;
- a test is then applied to separate the auto–term TF points from cross–term TF points by applying an appropriate testing criterion based on the normalized trace function of the STFD matrices;
- vector clustering to obtain the TF signatures of sources, hence their TFDs. This is done by observing that the auto-term STFD matrices of the same source signal have the same principal eigenvector (which corresponds to the considered source spatial signature);
- and recovery of original source waveforms from their estimated TFDs using TF synthesis.

Next, we propose to improve the separation performance of such TFD–based algorithms by using a component extraction procedure exploiting the linear–features of considered FM–like signals.

3. PROPOSED UBSS ALGORITHM

To achieve UBSS, we introduce here a four–step approach consisting of:

- Computation and spatial averaging of the observed signal TFDs;
- Image component extraction to separate all signal components;
- Components classification to group together components belonging to the same multicomponent source signal;
- Time frequency signal synthesis to recover the original source waveforms.

3.1. Time frequency signal analysis and spatial averaging

The discrete-time form of the Cohen's class of TFDs, for a signal $x(t)$, is given by [9]

$$D_{xx}(t,f) = \sum_{l=-\infty}^{\infty}\sum_{k=-\infty}^{\infty} \phi(k,l)\times x(t+k+l)x^*(t+k-l)e^{-j4\pi fl} \tag{4}$$

where t and f represent the time index and the frequency index, respectively. The kernel $\phi(k,l)$ characterizes the distribution and is a function of both the time and lag variables. The cross-TFD of two signals $x_1(t)$ and $x_2(t)$ is defined by

$$D_{x_1x_2}(t,f) = \sum_{l=-\infty}^{\infty}\sum_{k=-\infty}^{\infty} \phi(k,l)\times x_1(t+k+l)x_2^*(t+k-l)e^{-j4\pi fl} \tag{5}$$

Expressions (4) and (5) are now used to define the following data *spatial time–frequency distribution* (STFD) *matrix*,

$$\mathbf{D_{xx}}(t,f) = \sum_{l=-\infty}^{\infty} \sum_{k=-\infty}^{\infty} \phi(k,l) \times \mathbf{x}(t+k+l)\mathbf{x}^H(t+k-l)e^{-j4\pi fl} \quad (6)$$

where $[\mathbf{D_{xx}}(t,f)]_{ij} = D_{x_i x_j}(t,f)$, for $i,j = 1,2,\ldots,m$ and $\mathbf{x}^H$ denotes the conjugate transpose of $\mathbf{x}$.

Under the linear data model of equation (1) and neglecting the noise terms, the STFD matrix defined in (6) takes the following structure:

$$\mathbf{D_{xx}}(t,f) = \mathbf{A}\mathbf{D_{ss}}(t,f)\mathbf{A}^H$$

where $\mathbf{D_{ss}}(t,f)$ is the source TFD matrix whose entries are the auto– and cross–TFDs of the sources.

To have a 'clean' distribution (i.e., a distribution that can reveal the features of the signal as clearly as possible without any 'ghost' component), we did use a newly developed high resolution quadratic TFD called the B–distribution [21]. In addition, we did use a spatial averaging [20] that mitigates further the sources cross–terms by a factor depending on their spatial signatures angle (see [20] for more details). More precisely, we compute the averaged TFD (on which line detection is applied) as:

$$D(t,f) = \text{Trace}(\mathbf{D_{xx}}(t,f)) = \sum_{l=1}^{m} D_{x_l x_l}(t,f) \quad (7)$$

3.2. Image–component extraction

The component–extraction method is divided into two main steps: (i) line detection giving local binary detection of the potential linear structures (segments), and (ii) global optimization giving a set of labeled components. Due to the scope of the paper, we only give a brief review of the method. Additional information, such as statistical behavior and typical values for thresholds, can be found in [16] and references therein. Because of the particularity of the TFD image, a preprocessing is needed before applying the component extraction procedure as explained below.

3.2.1. Preprocessing

The preprocessing consists first of the transformation of the TF image onto a real positive-valued image by forcing to zero all negative values[1] of the TFD and by using a gray scale in the range [1, 256]. Also, line detectors are usually limited to a line width of 5 pixels. If the researched components do not respect this limit (which is usually the case for a TF image), an image subsampling by block–averaging is applied to reduce the pixel size. Despite the blurring effect, this filter presents the advantage of reducing the noise in the TF image. Moreover, as the TF image is unisotropic (i.e., it contains horizontal lines as can be observed in Figure 1), this image downsampling (see Figures 3-f and 4-f) removes this particular feature of the TF image.

[1] Negative values correspond to undesired cross-terms or noise.

3.2.2. Line detection: Local optimization

Line detection is done at the pixel level by determining whether a pixel belongs to a line crossing it along a particular direction. Given a pixel x_0 and a direction $d_k \in \{d_1,\ldots,d_{N_d}\}$ ($N_d = 8$, typically). Three regions associated with x_0 and d_k are then set up as shown in Figure 2 with μ_i being the averaged amplitude (in terms of intensity). The response between two regions i and j is defined through their contrasts $c_{ij} = \mu_i/\mu_j$ as in (8a), or through their cross–correlation coefficients as in (8b):

$$r_{ij} = 1 - \min\{c_{ij}, c_{ji}\}, \quad (8a)$$

$$\rho_{ij} = \left(1 + (n_i + n_j)\frac{n_i\gamma_i^2 c_{ij}^2 + n_j\gamma_j^2}{n_i n_j (c_{ij}-1)^2}\right)^{-1/2} \quad (8b)$$

where, for region i, n_i is the number of pixels and γ_i is the variation coefficient (ration of standard deviation and mean). The detector is then defined by the minimum response of the filter on both sides of the structure:

$$r = \min\{r_{01}, r_{02}\} \gtrless \epsilon_r \quad (9a)$$

$$\rho = \min\{\rho_{01}, \rho_{02}\} \gtrless \epsilon_\rho \quad (9b)$$

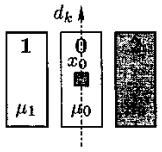

Figure 2: Regions associated with pixel x_0 and direction d_k.

A line passing x_0 along direction d_k is *detected* when the filter response is higher than the decision threshold ϵ_r (or ϵ_ρ). In practice, the line detector defined by (9a) is less accurate, whereas, the one defined by (9b) is sensitive to the threshold. Therefore, a combined binary detector was proposed using an associative symmetrical sum below:

$$\sigma(\tilde{r},\tilde{\rho}) = \frac{\tilde{r}\tilde{\rho}}{1-\tilde{r}-\tilde{\rho}+2\tilde{r}\rho} \gtrless 0.5, \qquad \tilde{r},\tilde{\rho} \in [0,1] \quad (10)$$

where $\tilde{r}$ and $\tilde{\rho}$ are the normalized, to the range of $[0,1]$, of r and ρ according to: $\tilde{r} := \max\{0, \min\{1, r + 0.5 - \epsilon_r\}\}$ (similarly for $\tilde{\rho}$). The detector in (10) is chosen because it is indulgent disjunctive for $\tilde{r},\tilde{\rho} > 0.5$, and conjunctive for $\tilde{r},\tilde{\rho} < 0.5$.

Further processing on the line–detected pixels to form segments is performed by first suppressing the isolated pixels, which are not closed (in terms of direction) to any other

neighboring pixels, and then linking pixels closed (in terms of direction and spatial distance) to each other.

3.2.3. Road detection: global optimization

Given a set of locally detected segments found in the previous step, this step introduce *global* constraints on the shape of the linear features to connect segments that correspond spatially to a larger feature in the whole image, i.e. to connect parts of a true "road", while suppressing falsely detected segments. The connection scheme is globally optimized using *Markov random field* (MRF)–based model for roads [16]. In this paper, the underlying MRF model is defined on a graph structure as follows.

MRF model on graphs [17]: Let $\mathcal{G} = \{\mathcal{V}, \mathcal{E}\}$ be a *graph*, where $\mathcal{V} = \{s_1, \ldots, s_N\}$ is the set of *vertices* (nodes), and $\mathcal{E}$ is the set of *edges* connecting them. Suppose that there exists a *neighborhood system* $\mathcal{N} = \{n(s_1), \ldots, n(s_N)\}$ on $\mathcal{G}$ where $n(s_i)$ is the set of all the nodes in $\mathcal{V}$ that are neighbors of s_i such that (i) $s_i \notin n(s_i)$, and (ii) $s_j \in n(s_i) \Leftrightarrow s_i \in n(s_j)$. Let $\mathcal{X} = \{x_1, \ldots, x_N\}$ be a family of random variables defined on $\mathcal{V}$, then $\mathcal{X}$ is called a *random field* where x_i is the random variable associated with s_i. We say $\mathcal{X}$ is an MRF on $\mathcal{G}$ with respect to (w.r.t.) $\mathcal{N}$ iff[2]:

1. $p(\mathbf{x}) > 0$ for all realizations $\mathbf{x} \in \Omega$, and
2. $p(x_i | x_j, s_j \neq s_j) = p(x_i | x_j, s_j \in n(s_i))$

A *clique* c is a subset of $\mathcal{V}$ for which every pair $(s_i, s_j) \in c$ are neighbors. Denote $\mathcal{C}(\mathcal{G}, \mathcal{N})$ the collection of all the cliques of $\mathcal{G}$ w.r.t. $\mathcal{N}$, the general functional form of the *pdf* of the MRF can be expressed as the following *Gibbs distribution*:

$$p(\mathbf{x}) = \frac{1}{z} \exp\left[-\mathcal{U}(\mathbf{x})\right] \tag{11}$$

where $\mathcal{U}(\mathbf{x}) = \sum_{c \in \mathcal{C}} V_c(\mathbf{x})$ is called the *Gibbs's energy function*, V_c is called a *potential* depending on c, and z is a normalizing constant.

We now apply the above MRF model on graphs to our problem of road detection. The nodes s_i are the detected segments. The set $\mathcal{E}$ contains "possible" connections. A possible connection is verified by: (i) it links two end–points (e_i^k, e_j^l; $k, l \in \{1, 2\}$) of two different segments, (ii) the end–points are closed enough, and (iii) the alignment of the two segments is acceptable. The neighborhood of s_i is $n(s_i) = \{s_j : \exists (k, p), e_j^p = e_i^k, j \neq i\}$. The cliques are all subsets of $\mathcal{V}$ sharing an extremity, including singletons and cycles of three segments. Road detection consists in identifying the nodes that belong to a road, i.e. in labeling the graph, resulting a label random field: $\mathcal{L} = \{L_1, \ldots, L_N\}$ ($L_i = 1$ if s_i belongs to a road, and $L_i = 0$ otherwise). $\mathcal{L}$ takes its values in Ω, the set of all (2^N) possible configurations (realizations).

[2] $p(\mathbf{x}) = P(\mathcal{X} = \mathbf{x})$.

The result of road detection is defined as the most probable configuration for $\mathcal{L}$ given the observation[3] $\mathcal{D} = \{D_1, \ldots, D_N\}$ for the segments of $\mathcal{V}$. The solution, then, corresponds to the maximum of the conditional probability distribution of $\mathcal{L}$ given $\mathcal{D}$, using Bayesian rule, as:

$$p(\mathcal{L}|\mathcal{D}) = \frac{p(\mathcal{D}|\mathcal{L})\, p(\mathcal{L})}{p(\mathcal{D})} \tag{12}$$

All the probability distributions $p(\mathcal{D}|\mathcal{L})$, $p(\mathcal{L})$ and $p(\mathcal{D})$ follow the Gibbs distribution in (11). Details of their corresponding energy functions and clique potentials can be found in [16].

The output of the road detection step is the set of roads with their associated segments. A simple snake–based method is then used to visually joint the labeled segments [16]. In the resulting TF plane (having converted from the above output image), each extracted road is now called a *source component* belonging to some particular source signal.

3.3. Component classification

In [15], it has been observed that two auto–term points (t_1, f_1) and (t_2, f_2) corresponding to the same source $s_i(t)$ are such that:

$$\mathbf{D_{xx}}(t_1, f_1) = D_{s_i s_i}(t_1, f_1)\mathbf{a}_i\mathbf{a}_i^H,$$
$$\mathbf{D_{xx}}(t_2, f_2) = D_{s_i s_i}(t_2, f_2)\mathbf{a}_i\mathbf{a}_i^H,$$

which means that $\mathbf{D_{xx}}(t_1, f_1)$ and $\mathbf{D_{xx}}(t_2, f_2)$ have the same principal eigenvector $\mathbf{a}_i$ ($\mathbf{a}_i$ being the i–th column vector of $\mathbf{A}$). The idea of the proposed component classification procedure is to group together components associated with the same spatial direction (estimated as the averaged value over all component points of the principal eigenvectors of the corresponding STFD matrices) representing a particular source signal.

For each extracted component C, one estimate the corresponding spatial direction as:

$$\mathbf{a}_C = \frac{1}{\#\mathcal{I}_C} \sum_{i \in \mathcal{I}_C} \mathbf{a}(t_i, f_i)$$

where $\mathcal{I}_C$ denotes the set of points of component C, $\#\mathcal{I}_C$ denotes the number of points in $\mathcal{I}_C$ and $\mathbf{a}(t_i, f_i)$ is the estimated principal eigenvector of the i–th component point STFD matrix $\mathbf{D_{xx}}(t_i, f_i)$. These vectors are then clustered into different classes using the clustering algorithm in [15].

3.4. Time frequency signal synthesis

The source signatures, after a proper clustering step, can be reconstructed to obtain their original waveforms through the use of TF synthesis. We have applied in our simulations a

[3] D_i is deduced by averaging $\sigma(\tilde{r}, \tilde{\rho})$ of all pixels in segment s_i.

classical but seminal algorithm (without any TF masking), proposed by Boudreaux–Bartels *et al.* [18]. Other synthesis algorithms can be found in [9, 19]. The successful recovery of original signal waveforms depends on the signal type, choice of TFD, the robustness of vector clustering step, and the performance of the time–frequency (TF) synthesis algorithm itself.

On the other hand, instead of using TF synthesis, we may apply the time–varying notched filter approach as shown in [22].

4. SIMULATED EXPERIMENT

To illustrate the performance of the proposed algorithm we present here two simulation examples corresponding to the separation of $n = 3$ multicomponent FM sources using $m = 2$ mixtures (outputs). All components are of constant amplitude equal to one and additive noise power is set to $0dB$. In the first case (Figure 3), all sources are chirp signals (two of them are monocomponent chirps and the third one is a two–components chirp signal) and in the second case (Figure 4), one of the sources is a monocomponent quadratic FM signal.

Although no thorough statistical analysis has been done so far, we can observe from these results very good estimation performances that can be confirmed and reinforced in future works by more detailed performance studies.

5. CONCLUSION

This paper has presented a new approach for blind separation of nonstationary sources using their TFDs. This approach is based on a 'line detection algorithm' to extract separately all the components, using a spatially averaged 'cross-terms free' time-frequency distribution (TFD), of the observed signal. The source spatial signatures are then used to group together components of the same source signal through a vector clustering procedure. Simulation examples are provided to illustrate the performances of the proposed method for the underdetermined blind separation of nonstationary FM signals. The method developed in this paper represents a new research direction for solving the UBSS problem. Still many problems remain under investigation including improvements of the vector clustering steps, a detailed performance analysis to better assess the advantages and limits of this new approach, comparisons with the method in [15], and extensions to the convolutive mixture case.

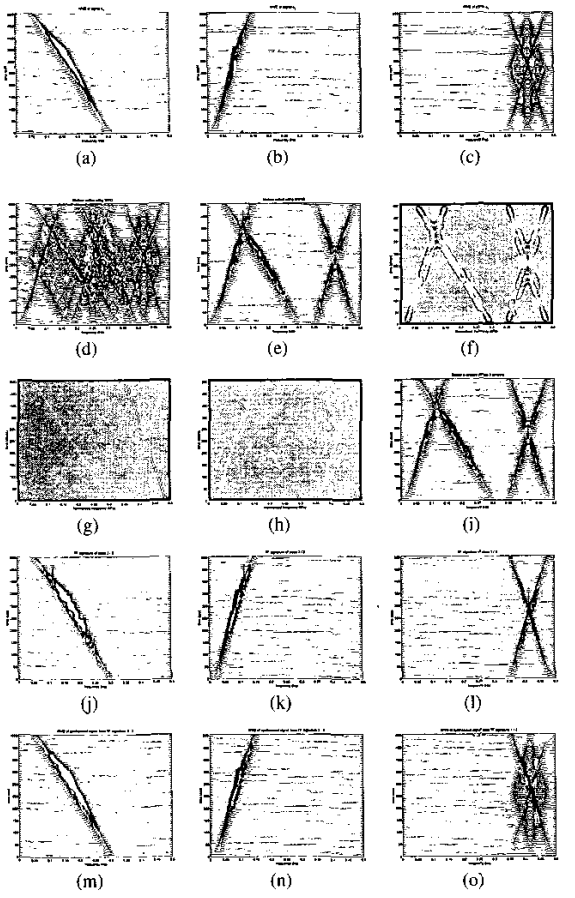

Figure 3: Experiment 1: (a–c) WVD of $s_1(t)$, $s_2(t)$, $s_3(t)$; (d,e) spatial–averaged TFD of the mixture outputs using WVD and MWVD; (f) convert STFD mixture to image; (g-h) extraction of source components using image processing; (i) auto–term points of known components; (j–l) TFD estimates of the sources; (m–o) TFD of estimated sources after TF synthesis.

6. REFERENCES

[1] J. F. Cardoso, "Blind signal separation: Statistical principles," *Proc. IEEE*, 9:2009–2025, Oct. 1998.

[2] *Series of Proceedings of the International Workshops on Independent Component Analysis (ICA)*, 1999, 2000, 2001, 2002.

[3] P. Comon, "Independent component analysis: A new concept?," *Signal Processing*, 36:287–314, 1994.

[4] X.-R. Cao and R.-W. Liu, "General approach to blind source separation," *IEEE Trans. Sig. Proc.*, 44:562–571, Mar. 1996.

[5] T.-W. Lee, *Independent Component Analysis: Theory and Applications*. Boston: Kluwer Academic, 1998.

[6] V. Zarzoso and A. K. Nandi, "Blind source separation," in *Blind Estimation Using Higher-Order Statis-*

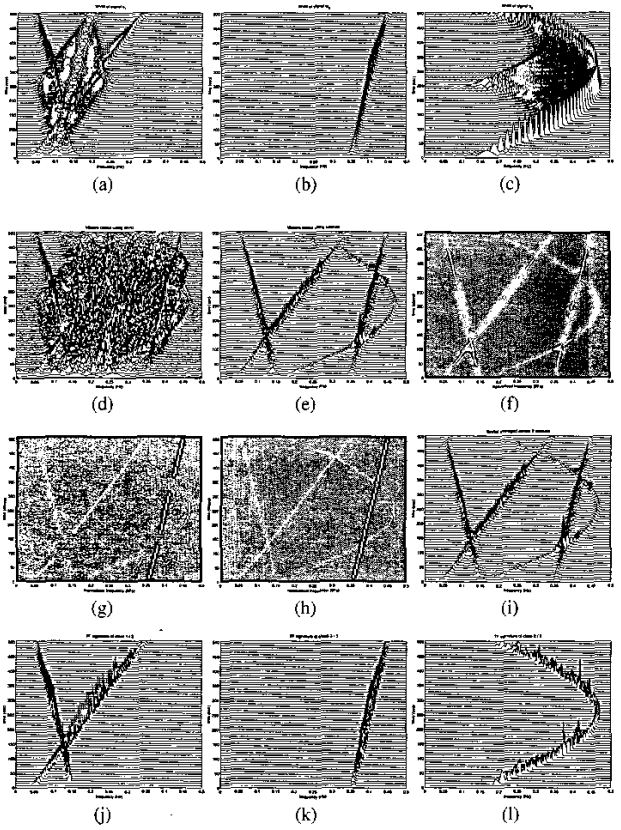

Figure 4: Experiment 1: (a–c) WVD of $s_1(t)$, $s_2(t)$, $s_3(t)$; (d,e) spatial–averaged TFD of the mixture outputs using WVD and MWVD; (f) convert STFD mixture to image; (g-h) extraction of source components using image processing; (i) auto–term points of known components; (j–l) TFD estimates of the sources

tics (A. K. Nandi, ed.), 167–252, Boston: Kluwer Academic, 1999.

[7] A. Belouchrani and M. G. Amin, "A new approach for blind source separation using time-frequency distributions," in *Proc. SPIE Conf. Advanced algorithms and Architectures for Signal Processing*, (Colorado), 1996.

[8] A. Belouchrani and M. G. Amin, "Blind source separation based on time-frequency signal representations," *IEEE-T-SP*, 46:2888–2897, Nov. 1998.

[9] B. Boashash, ed., *Time-Frequency Signal Analysis: Methods and Applications*. Australia: Longman Cheshire, 1992.

[10] P. Comon, "Blind channel identification and extraction of more sources than sensors," in *Proc. SPIE*, vol. 3461, (San Diego), July 1998.

[11] A. Belouchrani and J.-F. Cardoso, "Maximum likelihood source separation for discrete sources," in *EUSIPCO*, 1994.

[12] A. Taleb and C. Jutten, "On underdetermined source separation," in *ICASSP'99*, 3:1445–1448, 1999.

[13] K. I. Diamantaras, "Blind separation of multiple binary sources using a single linear mixture," in *ICASSP'2000*, (Turkey), 5:2657–2660, June 2000.

[14] A. Jourjine, S. Rickard, and O. Yilmaz, "Blind separation of disjoint orthogonal signals: demixing n sources from 2 mixtures," in *ICASSP*, (Turkey), 5: 2985–2988, June 2000.

[15] L.-T. Nguyen, A. Belouchrani, K. Abed-Meraim, and B. Boashash, "Separating more sources than sensors using time–frequency distributions," in *ISSPA'01*, (Malaysia), 2:583–586, Aug. 2001.

[16] F. Tupin, H. Maître, J.-F. Mangin, J.-M. Nicolas, and E. Pechersky, "Detection of linear features in SAR images: Application to road network extraction," *IEEE Trans. Geosci. Rem. Sens.*, 36(2):434–453, 1998.

[17] J.W. Modestino, and J. Zhang, "A Markov random field model–based approach to image interpretation," *IEEE Trans. Patt. Anal. Mach. Intel.*, 14(6):606–615, Jun. 1992.

[18] G.F. Boudreaux-Bartels and T.W. Marks, "Time varying filtering and signal estimation using Wigner distributions", *IEEE Tr. on ASSP*, vol. 34, pp. 422–430, Mar. 1986.

[19] A. Francos and M. Porat, "Analysis and synthesis of multicomponent signals using positive time-frequency distributions," *IEEE-T-SP*, vol. 47, pp. 493–504, Feb. 1999.

[20] M.G. Amin, W. MU and Y. Zhang, "Spatial and time-frequency signature estimation of non-stationary sources", *Proc: SSP Workshop (Singapore)*, pp. 313–316, Aug. 2001.

[21] B. Barkat and B. Boashash, "A High-Resolution Quadratic Time-Frequency Distribution for Multicomponent Signals Analysis", *IEEE-T-SP*, 49(10), Oct. 2001.

[22] M.G. Amin, "Interference mitigation in spread spectrum communication systems using time-frequency distributions", *IEEE-T-SP*, vol. 45, no. 1, pp. 90–101, Jan. 1997.